




Investigating the possibility of using second-life batteries for grid applications

Abdulla Rahil¹  | Eduard Partenie¹ | Mark Bowkett¹ | Mian H. Nazir¹  | Muhammad M. Hussain² 

¹The Centre for Automotive and Power Systems Engineering (CAPSE), Faculty of Engineering, Computing and Science, University of South Wales, Pontypridd, Wales, UK

²Electrical & Electronic Engineering Department, Faculty of Engineering, Computing and Science, University of South Wales, Pontypridd, Wales, UK

Correspondence

Abdulla Rahil, The Centre for Automotive and Power Systems Engineering (CAPSE), Faculty of Engineering, Computing and Science, University of South Wales, Pontypridd, CF37 1DL Wales, UK.
Email: Abdulla.rahil@southwales.ac.uk

Abstract

This paper investigates the potential for use of batteries from retired plug-in hybrid electric vehicles (PHEVs) in specific grid applications. In this study, project, a reference capacity test was performed to check the state of health, state of charge (SOC) and battery durability of a PHEV battery, and the pack was then tested under duty cycles for different grid applications to determine whether it would satisfy such applications in technical terms. The duty cycles considered are peak shaving, frequency regulation, photovoltaic (PV) smoothing and renewable energy firming. The data show that the battery can satisfactorily fulfil the requirements of peak shaving applications in terms of stability and battery retention capacity, and that the requirements of the frequency regulation service are also partially met. The untracked time for the battery signal was 4% (slightly exceeding the condition set for passing the tracking test, which is 2%). The SOC and temperature were within permitted limits. The battery, however, did not achieve good performance for PV smoothing or renewable energy (RE) firming. The untracked times were 14% and 11% for PV smoothing and RE firming, respectively (greatly exceeding the 2% condition for passing the tracking test). The SOC and temperature for the PV smoothing were within acceptable limits. The pack failed to complete the RE firming cycle as the SOC reached maximum safety limits after 6 h and 23 min, whereas the duty cycle is 10 h long.

KEYWORDS

frequency regulation, peak shaving, reference capacity test, second-life batteries

1 | INTRODUCTION

Electric vehicle (EV) numbers on the road network have risen exponentially in recent years, with more than 7 million EVs as of 2019.¹ Predictions of future rises in EV numbers suggest that by 2030, between 100 and 200 GWh will be available through batteries nearing their retirement age

as they become unable to fulfil the specified requirements for EV use. This is approximately equal to the volume of batteries currently produced each year.¹ Frequently, used batteries are categorised as hazardous waste due to the toxicity of their components, high reactivity and flammability. Thus, there is increasing social concern around the potential risks to the environment, which will occur in

This is an open access article under the terms of the Creative Commons Attribution License, which permits use, distribution and reproduction in any medium, provided the original work is properly cited.

© 2022 The Authors. *Battery Energy* published by Xijing University and John Wiley & Sons Australia, Ltd.

the disposal of this number of used battery units. On the other hand, this retired battery stock has also been viewed as a possible resource that can be utilised to provide value. Central to this vision is the need to establish financial and technological flows through which this resource can be refurbished, reused and recycled. Practices already introduced for dealing with used batteries include a complex process to recycle the valuable materials in batteries through extraction, around which an industry is emerging.² In recent years, there has been growing attention paid to developing uses for used cell, module and pack batteries that are suitable for further uses: the growth of such approaches should eventually decrease energy storage costs and promote more extensive use of renewables within power grids.³

At present, the most frequently used battery type for the electric vehicle market is the lithium-ion battery (LIB). This is based on LIBs' longevity, power density and high energy, and the fact that their price has reduced considerably across the past 10 years. Several million hybrid electric vehicles (xEVs) and EVs using LIBs have been purchased, with considerable increases in the numbers of such vehicles on the road being predicted for the near future as the vehicle sector increasingly turns to electric-powered vehicles. Avicenne Energy¹ reports that LIBs are the fastest-growing and most investment-attracting part of the sector. Globally, sales of LIBs rose on average by 16% annually between 1996 and 2016, when the market for LIB cells was valued at more than \$20 billion, with predictions that this will rise to around \$40 billion by 2025. From this figure, over \$15 billion is predicted to derive from xEVs and EVs. For the United States alone, 1.4 million sales of EVs are predicted for 2035, according to the US Energy Information Administration (EIA). Such increases in demand would lead to a high volume of LIBs, which had ended their lifespan for EV use, with predictions of 1 million spent packs in 2030, rising to 1.9 million 10 years later. Cumulatively, this translates into up to 21 million LIB packs reaching their end-of-life phase in the period 2015–2040.² While EV LIBs have a predicted minimum lifespan of between 8 and 10 years, it is essential to plan for end-of-life uses as soon as possible, so that the necessary infrastructure can be prepared to deal with the higher-volume recycling activities, which will be needed. There are a number of factors that make it essential to recycle these LIB packs. This activity provides protection against changes in the price of materials, allows unevenness in manufacturing, distribution and materials sources to be compensated for, as well as responding to conditions in transportation.

Authors in Ref. 4 found that solar and storage systems of an appropriate size for utilities would make a profit where used batteries cost less than 60% of the cost of new batteries. Neubauer et al. find profitability in area regulation, and probable profitability for power quality

in electricity services, integrating wind power into grids, deferring upgrades to distribution and short-term transmission. Meanwhile, according to Song et al., wind farm applications of second-life battery units are not economic presently.⁵ Further research work supports the profitability of photovoltaic (PV) energy production along with managing household demand.^{6–8} On the other hand, Heymans et al. consider that a favourable environment would be needed in order for load levelling applications to achieve profitability.⁹ Although the research discussed above evaluates second life batteries' potential for profitable applications, it does so based only on previous predictions of the cost of acquiring such batteries and how they will perform, which means that significant factors are assumed without taking into account performance and prices in the market if technologies used to recondition batteries advance. The findings of a literature review on second-life energy storage conducted in 2019 identified that the price of a second-life EV battery varied between \$44 and \$180 per kWh.¹⁰

Neubauer et al. gave an estimation of the cost of repurposing EV LIB modules but determined the price at reselling through the multiplication of the purchase cost of an unused battery by the repurposed battery's health factor. Moreover, although a number of works estimate costs involved in systems using second-life batteries, no studies were found for this work that had assessed costs involved in applying reconditioning methods to enhance a second-purpose energy storage system (ESS).¹¹

Reconditioned, repurposed batteries have great potential for enhanced performance and therefore increased value. This study project assesses the economic viability of reconditioning batteries through a new technique based on the heterogeneous unifying battery (HUB) system. This approach aims to enhance state of health (SOH) uniformity within battery module cells while avoiding the requirement to take the module apart. Modelling of the economic features of this reconditioning approach took place for two separate cases: RGS, or reconditioning with grid services; and RES, or reconditioning through energy shuffle. This study makes a direct comparison between the HUB approach to reconditioning and conventional processes for repurposing batteries in which modules are sorted, generating battery packs (BPs) that have a comparable SOH.^{12,13} This study calculates resale prices following these two approaches before extending the economic analyses' systems parameters for the inclusion of power/energy services leveraging repurposed battery modules. Economic comparisons are made between the second-use batteries and unused LIBs in use in energy and power service settings.¹⁴ This involves comparing both performance and costs for each type of battery in a range of energy/power service uses. The study uses sensitivity analysis to evaluate

the need for research and development investments strategically seeking to develop the technology required for commercial application. This study makes an original contribution through assessing the economics, which underpins reconditioning of second-life batteries to enhance performance in comparison to conventional repurposing, using enlarged systems parameters in assessing grid ESS viability.¹⁵

2 | PACK DETAILS, TEST EQUIPMENT AND TEST PROCEDURE

2.1 | Pack details

The tested pack is a used plug-in hybrid vehicle (PHEV). The capacity of these new packs is 25 Ah. The pack consists of 84 cells in series. The mileage is not specified in vehicle history. The full details about the pack and the cells are presented in Table 1.

2.2 | Test equipment

A Bitrode FTF battery pack tester (Bitrode Corporation) was used to perform grid application duty cycles. It provides two channels with a current limit of up to 1000 A (4000 A in parallel connections) and multiple voltages ranging from 35 to 500 V/40 to 700 V/58 to 1000 V. It provides a voltage and current accuracy of $\pm 0.1\%$ full-scale. The data sampling rate is 10 ms (1 ms optional). The FTF was used for all grid application duty cycles, including peak shaving, frequency regulations (FR), PV smoothing, and RE firming. A 15 kW DC power supply from Delta Elektronika was used to perform the

reference capacity test. The current range of the 15 kW DC power supply is -30 to $+30$ A for the discharge and charge respectively and the voltage limit is 500 V. The current range can be extended by connecting up to six power supplies in parallel. This bidirectional power supply can be programmed and controlled remotely.¹⁶

2.3 | Test procedure

This paper will focus on the preparation step in terms of testing. First, a reference capacity test is performed to check the SOH and SOC. Second, the pack is tested based on different grid applications' duty cycles, such as peak shaving and frequency regulation, to determine the capability of the pack to fulfil these applications from a technical view.

2.3.1 | Reference capacity test

This test was performed on the pack to check the SOH and the actual available capacity remaining from its primary use in an EV. The pack was charged and discharged at various C-rates (1 C, 0.5 C [12.5 A] and C/5 [5 A]). C rate represents the exact charge capacity of the battery in Ah, of which only the quantity is used for the current rates. The battery charge capacity commonly cannot be realised only through constant-current charge or discharge. A constant-voltage stage might be required to achieve full charge or discharge.

Then the battery capacity and duty cycle round trip efficiency (RTE) were calculated. The capacity test was performed to determine an accurate and comparable cell capacity at various C-rates. During the charge cycle, the constant current charged the cells up to maximum voltage (V_{\max}) and maintained a constant voltage of V_{\max} until the current dropped to 0.05* rated capacity. Likewise, during the discharge cycle, the constant current discharged the cells to minimum voltage (V_{\min}) and maintained constant V_{\min} until the current dropped to 0.05* rated capacity. There was a rest of 30 min in between charge and discharge cycles to allow cells to return to electrochemical and thermal equilibrium conditions. The cycles were repeated three times.

2.3.2 | Peak shaving duty cycle

Determining peak shaving duty cycles, charging, resting, and discharging timeframes (in Figure 1: -1 , 0 and 1 , respectively represent charging, resting and discharge) means that a consistent application of duty cycle profile is possible across varied battery technology types,

TABLE 1 Pack/cell specification of the tested pack

	PHEV
Cell	Prismatic
Voltage (nominal)	312 V
Operation voltage	168–361 V
Current max.	250 A
Capacity	25Ah
Instant energy	6.9 kWh
Usable energy	5.8 kWh
Operating temperature	-40°C to $+60^{\circ}\text{C}$
Lowest cell voltage	2.5 V
Highest cell voltage	4.1 V

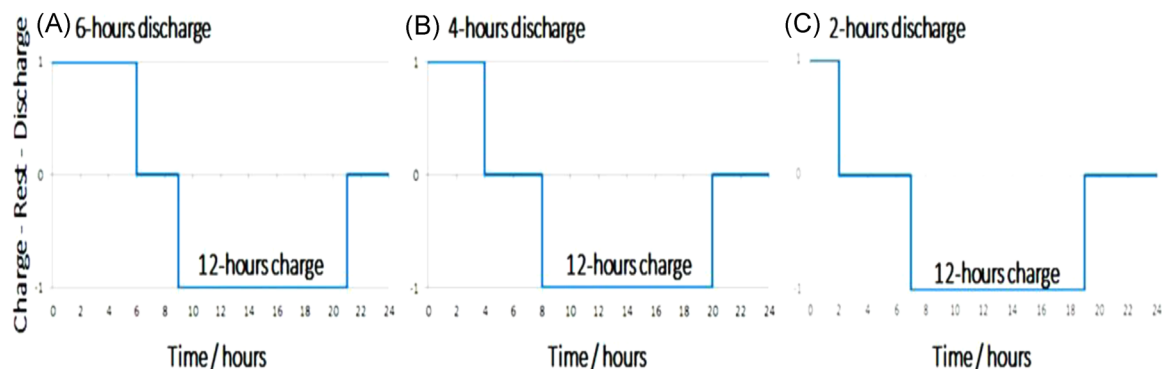


FIGURE 1 Peak-shaving duty cycles cover a 24 h period of time (X-axis) for each one of the duty cycles

systems sizes, condition, age and types.¹⁷ As reported in Conover et al.,¹⁷ the duty cycles have a 12-h overall charging time, with the time needed for discharge being 6 h for duty cycle A, 4 h for B and 2 h for C. Moreover, there is a postcharge time period for resting/standby, which brings each duty cycle to 24 h in total.

Before testing, each battery is charged at rated power to reach the maximum SOC as the starting point. The first stage in testing implements duty cycle A, discharging at a steady power rate to reach the manufacturer's prescribed minimum SOC point, at which point a resting/standby phase occurs, charging using constant power to reach the SOC higher limit, resting again and then a stage of rated power charging until the battery again reaches the maximum, starting SOC condition. This is followed by implementing duty cycle B and then C. Before starting duty cycles B and C, rated power is used to charge the batteries to the upper limit of SOC. After duty cycle C has been run, cells are returned to either the highest SOC or their starting SOC, where these differ. Due to the time restriction and limited access to the pack testing equipment, we opted to compress the duty cycles and reduce the charge window to 6 h rather than 12 h.

The recommendation from experts in this field¹⁷ is that the three duty cycles (A–C) should be run continuously; however, because of the institution's policy on health and safety, each cycle was run separately and during the daytime only, when it could be supervised (7:00 AM–9:30 PM), therefore each cycle took nearly 2 days to finish.

2.3.3 | Frequency regulation

FR services are contracted with a maximum power that an operator can provide through a window of time, and the grid operator then sends a signal for the storage operator to follow, up to a maximum of the contracted power value.¹⁷ Revenue is directly proportional to the peak power value contracted, so optimising it is a necessary goal when

providing regulation services. The inefficiency of the battery and converter systems requires that the operator be able to recharge the battery in operation, and a power signal may be asymmetric for some time, from hours to days, leading to a slow charge or discharge of the battery.

From 2012 to 2016, the Pacific Northwest National Laboratory (PNNL) and Sandia National Laboratories (SNL) in the United States worked to develop a testing protocol to allow consistent measurement and reporting of energy storage system performance.¹⁷ The protocol concerns applications within grid services, such as peak shaving, frequency regulation, microgrids, power quality and solar PV smoothing. The duty-cycle signal for frequency regulation applications of energy storage systems are specified for frequency regulation, as presented by SNL, with a detailed description available in Rosewater and Ferreira.¹⁸ The duty cycle was developed based on in-depth analyses conducted with data on frequency regulation control signals provided by a major independent operator of electricity systems in the East of the United States, PJM. Standard deviation, σ for daily frequency regulation signal was assessed as a suitable measure based on its aggressive character. It was also found that dynamic behaviour ranges in daily frequency regulation signals were able to be taken from any 2 h period.¹⁸ The findings were used to generate a 24-h duty cycle based on two energy-neutral time periods of 2 h each taken from the data from PJM. The first slice represented average σ per day across the year, while the other provided maximum daily σ in the same period. The composite cycle allows both nominal frequency regulation and performance in the face of rarely occurring extremes to be included when testing a sample. The structure of the composite duty cycle is shown below:

- Three average σ signals, 6 h
- One aggressive σ signal, 2 h

- Three average σ signals, 6 h
- One aggressive σ signal, 2 h
- Four average σ signals, 8 h

The normalisation of the duty cycle to the highest permissible power value permits scaling of the signal by users based on the sample's power rating. This normalised FR duty cycle is shown in Figure 2, along with the time integral, which indicates net energy. Here, positive energy/power indicates discharge to the power grid from storage, while negative energy/power indicates charging to storage from the grid.

The initial SOC should be set as per the specifications provided by the manufacturer and test instructions. In this case, the starting SOC of the test was 50%. The BP should be brought back to its initial SOC at the end of the duty cycle. Due to time restrictions and limited access to the lab resources, a 12-h cycle was applied instead of a continuous 24 h.

The BP ability to meet the signal for the FR duty cycle of the BP reflects the battery pack ability to track and follow the signal. The ability of the BP to track the reference signal should be recorded during the RTE duty cycle test. The measurements should be taken at every point in time that the ESS receives a change in the balancing signal. The sum of the absolute magnitudes of the difference between the balancing signal and BP power should be calculated using the following Equation (1).¹⁷

$$\sum |P_{\text{signal}} - P_{\text{bp}}|, \tag{1}$$

where the P_{signal} is the balancing signal and the P_{BP} is the BP power (W). In general, the overall percentage of the inability of the pack to track the signal should be less than 2%. This percentage can be calculated as in following equation¹⁷:

$$(P_{\text{signal}} - P_{\text{BP}}) \div P_{\text{signal}}. \tag{2}$$

The percentage may be different based on the application and customer request. The failure of the BP to track the signal can be computed as in the following equation¹⁷:

$$\begin{aligned} &\% \text{ of time signal tracked} \\ &= (\text{time signal is tracked (h)} \\ &\quad \div \text{duration of duty cycle (h)} \times 100). \end{aligned} \tag{3}$$

Equations (1)–(3) will be used to calculate the tracking signal percentage for the FR, PV smoothing and RE firming.

2.3.4 | PV smoothing

PV smoothing is the mitigation of rapid fluctuations in variable PV power output, by using BPs. The purpose of PV smoothing is to amend frequency variations and stability issues that can arise at both feeder and

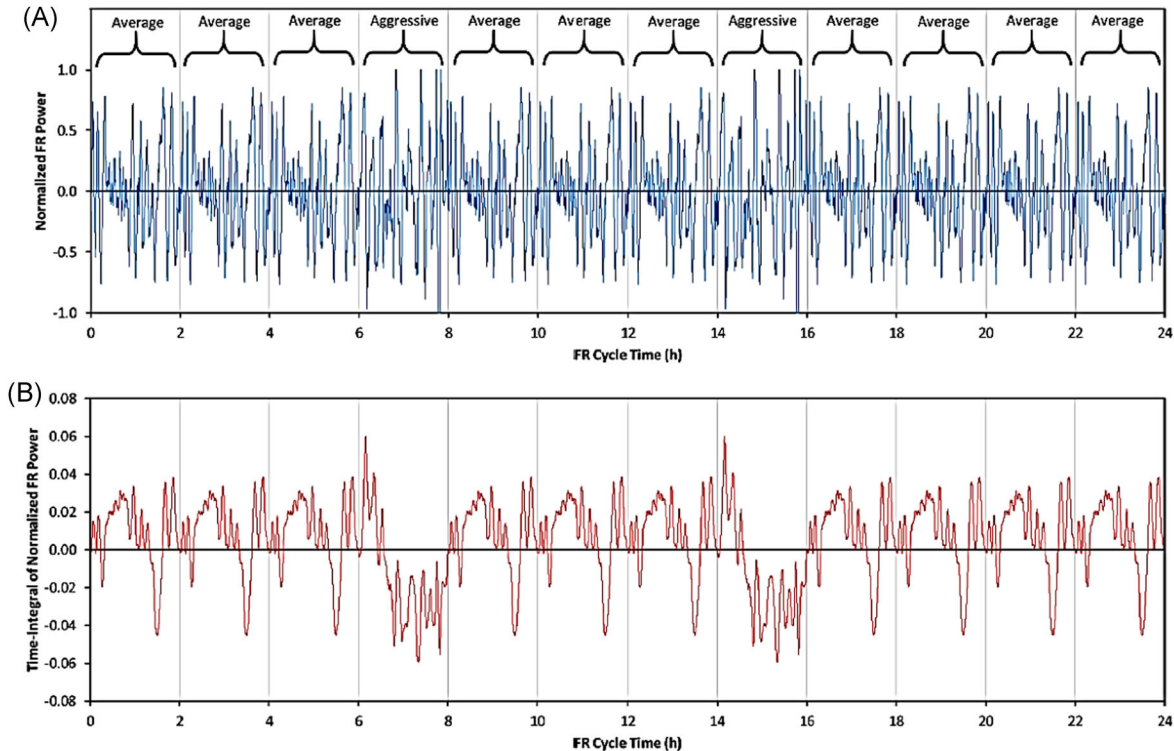


FIGURE 2 The normalised frequency regulations duty along with the time integral, which indicates net energy

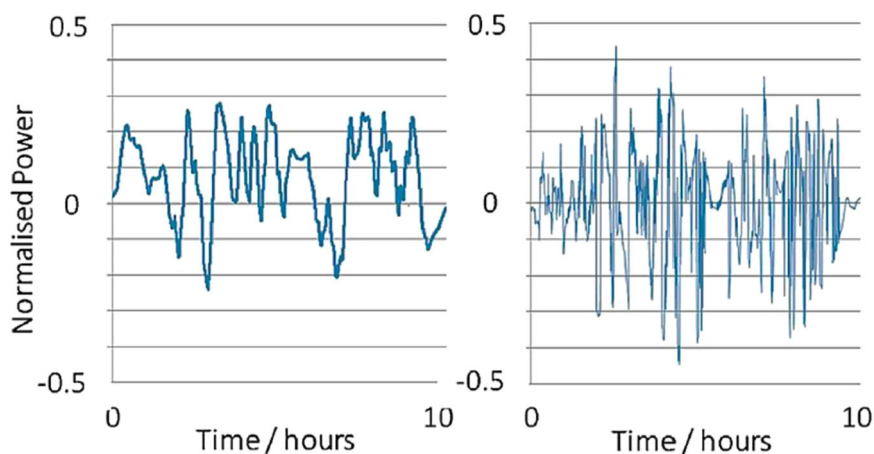


FIGURE 3 Duty cycles as normalised power: renewable firming (left) versus photovoltaic smoothing (right)

transmission levels in high-level PV scenarios, to help to respond to the ramp rate.¹⁷ At the feeder level, PV smoothing is performed to reduce voltage flicker and excursions outside permitted limits. At the transmission level, PV variability requires additional operating reserves to be set aside and can cause traditional generation to cycle more. The way by which the BP can provide smoothing of PV output power is the capacity to absorb or supply power at appropriate times, as requested by a control system, resulting in a less variable composite power signal at the feeder and/or transmission level.

The duty cycle was built on two main factors: the BP rated power and the load and supply profiles provided by our partners. The duty cycle was 10 h long with a 1-s signal, either charge or discharge. The duty cycle is less aggressive than the FR, simply because the sizing system of the PV plant should consider the variation between supply and demand to avoid more cost for large energy storage to tackle the issue of system sizing.

2.3.5 | Renewable energy (RE) firming

One of the applications of a BP is renewable firming, in which energy is provided to supplement renewable generation to produce stable power output for a given time. More specifically, the main function of renewables firming is to supply energy in cases where renewable generation falls below a certain limit. This process is applied to obtain stable power for a given number of hours.^{17,19} Normally, limits are established from forecasting nominal renewable power generation over the desired time window. Therefore, in the case of actual renewable generation during a given time, compensation from BP is provided in terms of forecast uncertainty. The

way a BP performs this compensation function is as follows: the BP discharges for periods of low renewable energy generation and charges when renewable generation exceeds this limit.

Although it can be necessary to provide outputs of stable power over many hours, the periods over which the BP attempts to firm power output are usually counted in the range of minutes, with 15 min being the most common duration considered. For limiting ramp rates over shorter periods, from 1 s to a minute, smoothing is used, while for longer periods ranging from 15 min to many hours, firming is mostly applied.

The duty cycles used here relating to renewable energy firming (REF) and photovoltaic smoothing (PVS), applied for energy and power smoothing, respectively, are based on Conover and colleagues,^{17,20} and are shown in Figure 3. For PVS, the design of the duty cycle is based on 1-h segments of PV power generation recorded across several days, before being added together to form a 10-h signal. Most segments making up this signal relate to PV variability, which ranges from medium variability to extremely strong variability constructing such composite signals allows for the capture of various time points across daily and annual cycles. In Ferreira et al.²⁰ the method for generating PVS duty cycle signals is described. To generate the duty cycle, PV power time series are normalised to the smoothing battery's rated power across a duration of 10 h in which a positive sign indicates power discharge and a negative sign indicates battery charging as a function of time (h). A similar procedure is used for constructing the duty cycle for REF, with the exception of the length of each time window, which ranges between minutes and hours as opposed to seconds to minutes, as described in detail in Conover et al.¹⁷

TABLE 2 Charge/discharge results at 12.5, 5 and 25 A

Reference test	Charge			Discharge		
	12.5	25	5	12.5	25	5
Current (A)	12.5	25	5	12.5	25	5
Voltage (V)	345	346.9	344.9	261.7	258.7	251
Capacity (% BMS, Ah calculation)	100, 23.3	96, 22	94.6, 22.5	0, 22.5	0.6, 22.5	0.7, 22.4
Temperature (°C)	26	17–23	17.5–19.5	20–28.5	22.5–29.5	22.5–29.5
RTE (%)	≈96.5	100	99.6	≈96.5	100	99.6
Time (h:min:s)	1:52:00	00:53:00	4:30:00	1:48:00	00:54:00	4:29:00

3 | RESULTS AND DISCUSSION

3.1 | Reference capacity test

In this study, the test was started by charging the pack at different currents: 5, 12.5 and 25 A. There was then a 30-min rest period before discharge took place at the same respective currents. Table 2 shows a summary of the test in terms of capacity, voltage during charge and discharge and temperature during charge and discharge. In short, the findings show that the pack was stable and demonstrated both high capacity and high RTE.

The charge and discharge time was almost 2 h, which is the expected time to complete a charge and discharge test at a C-rate of 0.5 C. There was also less drawn energy than injected energy, which might occur because of battery degradation, or the short rest period could have affected the Coulombic efficiency of the battery. Voltages during charge and discharge were close to the practical limits.

As a summary of the test, the capacity fluctuated between 22 and 23.5 Ah with a little capacity drop, which might be due to battery management system (BMS) practical voltage limits or battery degradation. Duty cycle RTE was high, giving a good sign about the robustness of the battery. The battery was stable in terms of charge and discharge voltages recommended by the battery manufacturer's limits under all C-rates.

3.2 | Peak shaving

3.2.1 | First cycle

The first cycle was charged at 4.2 A followed by approximately 2 h rest (in this case there was a long rest because we stopped testing at night), followed by discharge at 4.2 A. Due to the test limits, tester limits and practical voltage limits, the charge and discharge time was less than 6 h, while in the normal capacity test, charge and discharge time was around 50 min for the 1 C

test. The voltage threshold point for the charge and discharge was nearly 350 and 238 V, respectively.

A difference between the charge and discharge energy and then drop in RTE does not mean the pack is not suitable for this application as many factors could cause this drop in RTE, such as restricted voltage limits or a lengthy rest between charge and discharge; therefore, a rest of 30 min in between charge and discharge cycles is necessary to allow cells to return to electrochemical and thermal equilibrium conditions. The temperature during this cycle under charge and discharge was stable due to the low charge and discharge current as shown in Figure 4 (Table 3).

3.2.2 | Second cycle

In the second cycle, the charge window was the same (6 h) followed by a long rest due to the interruption at night, then the discharge window took place over 4 h. The summary of this cycle is given in Table 4, below.

The temperature of the two charge and discharge profiles is given in Figure 5.

3.2.3 | Third cycle

In this cycle, the charge window was the same as in A and B (6 h) followed by a long rest then the discharge window of 2 h was applied. A summary of this cycle is presented.

There are three main contributors to the voltage of batteries, including two electrical potentials from the electrodes' surface-level double layers, and the chemical potential differential among the electrodes. The double-layer potentials include both a contribution from equilibrium and from a finite ion transfer rate between the electrodes and the electrolyte. A battery's capacity refers to the quantity of ion transfer and is, therefore, a direct consequence of the electrodes' chemical structure and potentials.

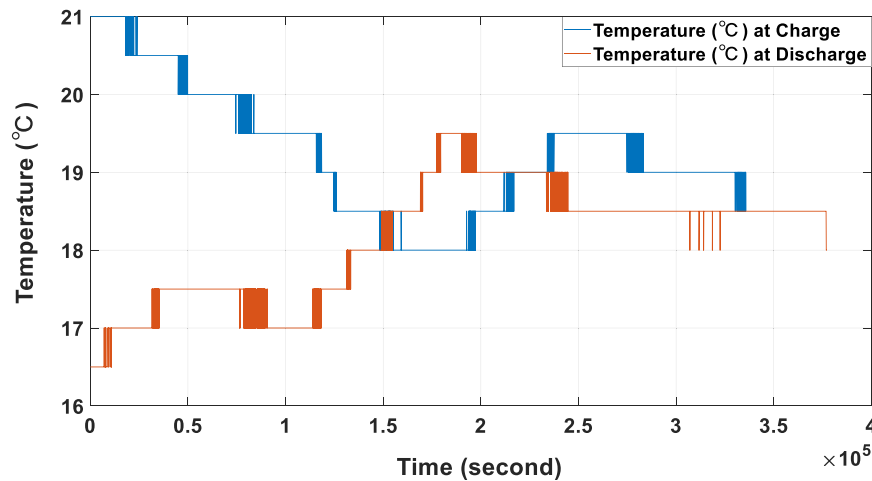


FIGURE 4 Temperature profile during the charge and discharge/cycle A

TABLE 3 Duty cycle A of peak shaving

Duty cycle	First cycle
Charge test time (h)	6.2
Real charge time (h:min)	4:47
Charge power (kW)	1.3
Charge energy (kWh)	6.7
Discharge test time (h)	6
Real discharge time (h:min)	4:58
Discharge power (kW)	1.3
Discharge energy (kWh)	6.4
Duty cycle roundtrip efficiency (%)	95.5

TABLE 4 Duty cycle B of peak shaving

Duty cycle	Second cycle
Charge test time (h)	6
Real charge time (h:min)	4:52
Charge power (kW)	1.4
Charge energy (kWh)	6.8
Discharge test time (h)	4
Real discharge time (h: min)	3:13
Discharge power (kW)	2
Discharge energy (kWh)	6.4
Duty cycle Roundtrip efficiency (%)	94

When a battery is charged to an identical voltage but using two distinct rates, higher-rate charging produces greater overpotential, leading to a smaller difference in chemical potentials (with the various voltage

contributions being summed) and therefore a lower level of ion transfer, with reduced capacity as a result.

The charge transferred through double layers contributes significantly to resistance. In high-resistance batteries, ions are transferred at a reduced rate, leading to greater overpotential for an identical charging rate. This will also lead to a reduced capacity.

A long rest between charge and discharge allows the pack to return to electrochemical and thermal equilibrium and offers better performance. The first and second cycles of peak shaving also help the pack to restore and refresh itself in terms of capacity. A higher discharge rate in the cycle (12.5 A) could also enable the pack to absorb more energy than in other cycles. The temperature profile during this cycle is given in Figure 6.

The data evidence that the pack is suitable for peak shaving applications. Additional tests can be included in peak shaving to verify compatibility with this application, such as response time and ramp rate. These tests will help us to see how fast the battery can respond and the ramp rate that can be achieved (Table 5).

3.3 | Frequency regulation

3.3.1 | The reference signal tracking

Figure 7 shows signal power and pack response power. There are minor differences between the signals that will affect the whole cycle, as demonstrated in the calculations below. The first part of the figure illustrates the first step, before applying the cycle that will bring the pack to 50% SOC.

From Equations (1)–(3), the percentage of the untracking time was 4% (exceeding the condition of passing the

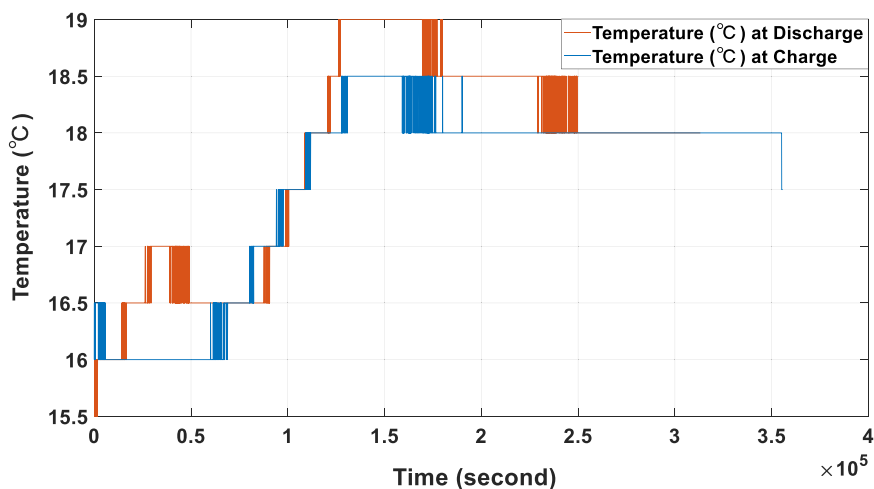


FIGURE 5 Temperature profile during the charge and discharge/cycle B

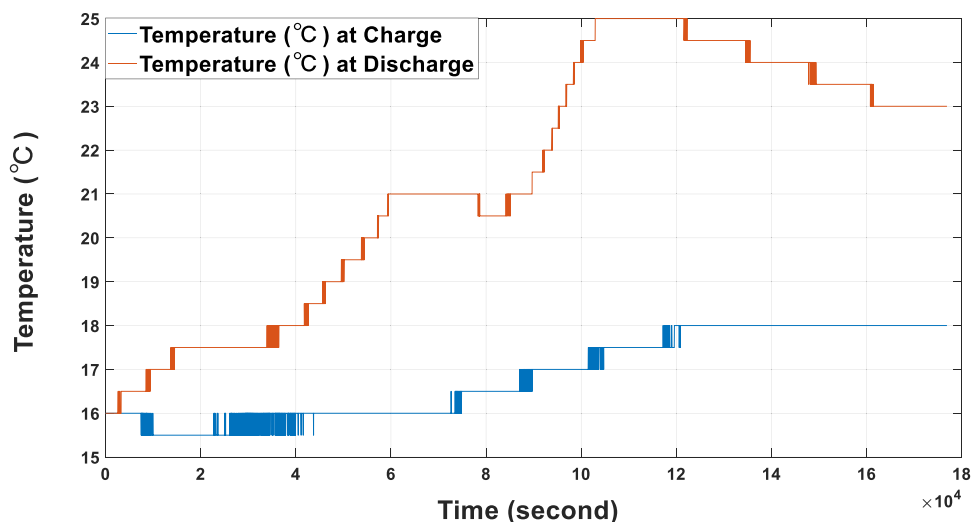


FIGURE 6 Temperature profile during the charge and discharge/cycle C

TABLE 5 Duty cycle C of peak shaving

Duty cycle	Third cycle
Charge test time (h)	6.0
Real charge time (h:min)	4:48
Charge power (kW)	1.3
Charge energy (kWh)	6
Discharge test time (h)	2
Real discharge time (h:min)	1:38
Discharge power (kW)	3.8
Discharge energy (kWh)	6.2
Duty cycle roundtrip efficiency (%)	100

tracking test, which is 2%). However, this test was not completed in its entirety since it was only performed for 12 h out of 24. In addition, running without temperature control could affect the battery's response since the temperature in the lab at the time of testing was cold (around 12°C), a fact that could affect the performance of the battery. Finally, the customer should decide the suitability of the pack with this percentage to be used for frequency regulation applications. The time of the tracking system as in Equation (3) above was

$$\% \text{ of time signal tracked} = (11.52 \div 12) \times 100 = 96\%.$$

As a result, the pack tracked the signal for nearly 96% of the total time.

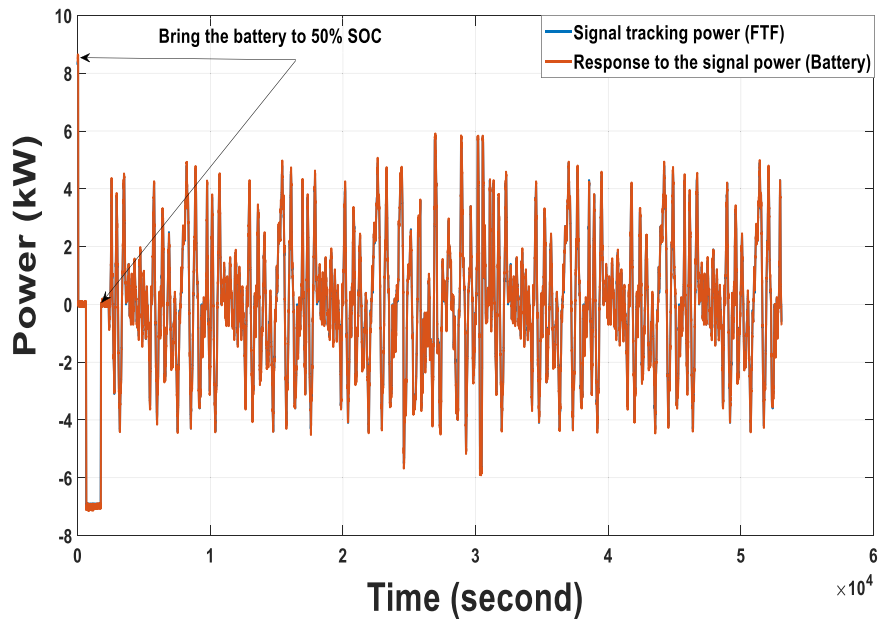


FIGURE 7 Power signal versus the response power from the pack

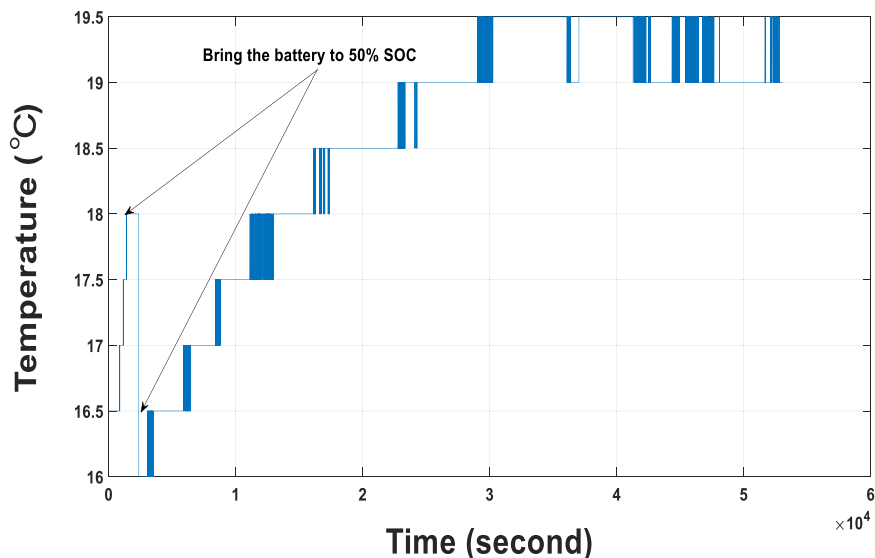


FIGURE 8 Temperature profile during the frequency regulations duty cycle

3.3.2 | Temperature and state of charge

Regarding the SOC, this should not fall below the desired limit specified by the battery manufacturer (between 20% and 92%). Figure 8 shows the temperature profile during the 12-h duty cycle, including the preparation of the pack before the test (bringing the pack to 50% SOC). The temperature change was between 15°C and 20°C. The tracking signal was not overly aggressive, as the usable rated power was set, and the battery tester limits also restricted the pack. The maximum drawing current recorded during charge and

discharge was close to 22 A (less than 1 C). However, a complete 24-h cycle in a different environment could lead to a significant increase in temperature since the test was run without temperature control.

Figure 9 compares the SOC with the signal tracking power. The SOC drops, although very slowly in the 12 h. Increasing the time of the duty cycle could lead to a clear drop in the SOC. In this test, the SOC dropped to 45%.

To sum up, the pack did not perform well in terms of tracking signals since the percentage of total time in which the signal was not tracked, at 4%, was slightly

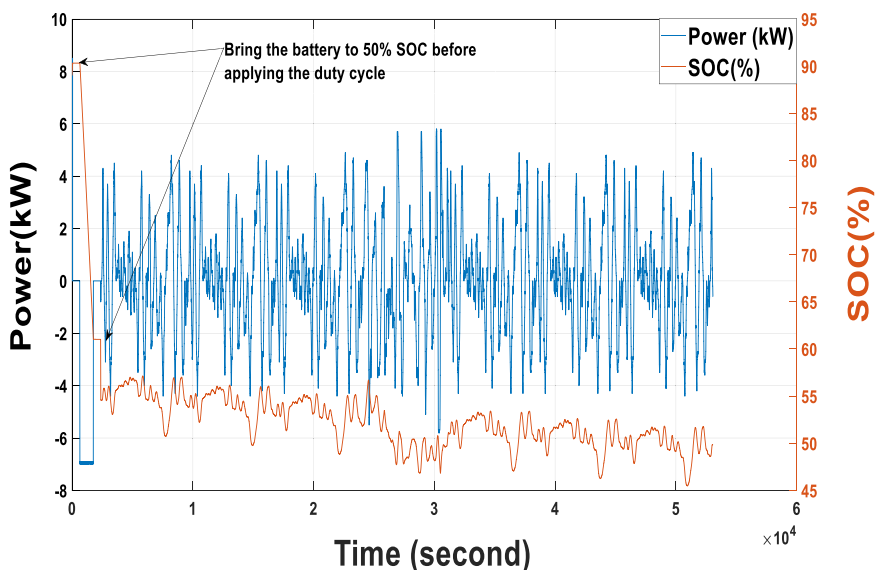


FIGURE 9 The SOC (%) versus power tracking signal (kW) during the frequency regulations duty cycle

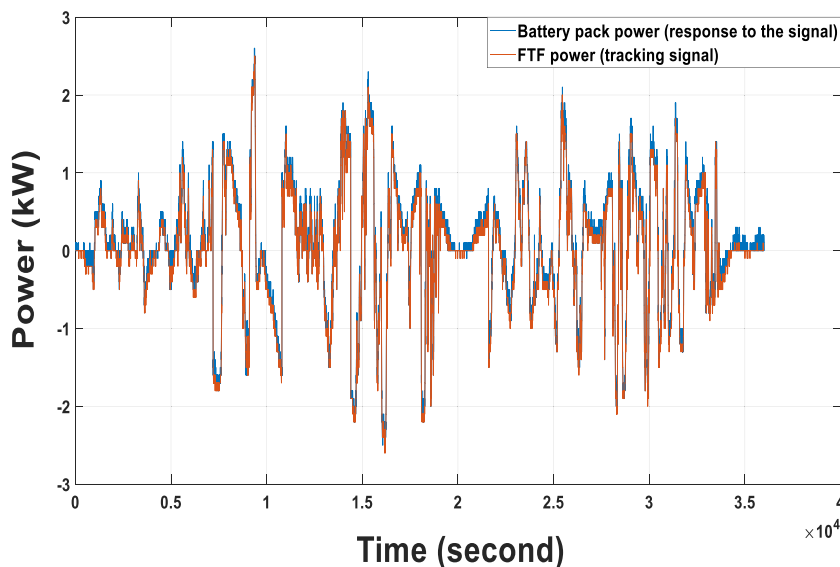


FIGURE 10 Battery pack power (kW) versus the signal power tracking (kW) under PV smoothing duty cycle

higher than the recommended limits. More duty cycles with aggressive tracking signals should be applied to assess the possibility of the pack tracking the power signal. Temperature and SOC were within satisfactory limits under the 12-h duty cycle period.

3.4 | PV smoothing

3.4.1 | The reference signal tracking

The duty cycle is normalised power with respect to the rated power of the BP over a period of 10 h, where a

positive sign means charge into the battery and a negative sign means discharge from the BP as a function of time in hours. The initial SOC is set as per the specifications of the manufacturer's and test instructions. Figure 10 shows how the battery responds to a generated signal simulating a PV smoothing application. In an ideal BP, the battery should fully track the signal. At some points, the battery under testing could not follow the tracking, while at some points the battery output exceeded the required tracking signal.

The percentage of untracking time compared to the whole cycle was 14%. This still fails to meet the desired recommended limit (2%). In terms of the tracked time, the BP was tracked for nearly 8.6 h out

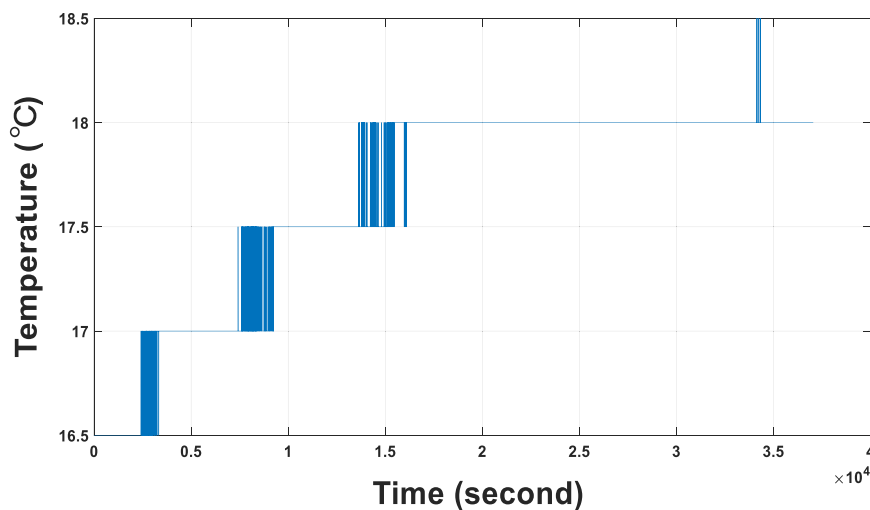


FIGURE 11 Temperature profile during the photovoltaic smoothing duty cycle

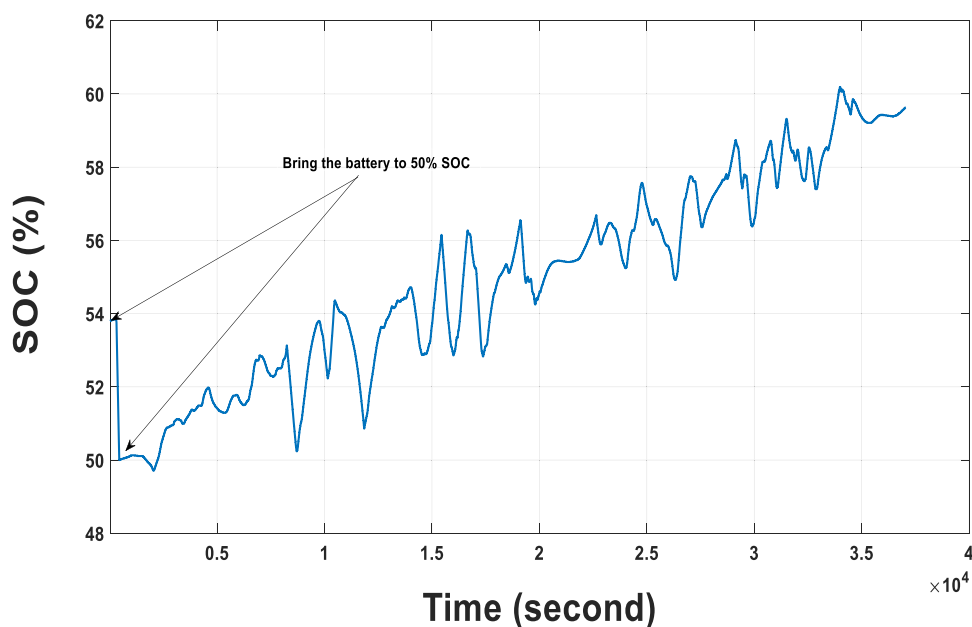


FIGURE 12 State of charge (SOC; %) during the photovoltaic smoothing duty cycle

of 10. In other words, nearly 1.4 h overall were without tracking.

$$\% \text{ of time signal tracked} = (8.6 \div 10) \times 100 = 86\%.$$

The pack was tracking the signal for nearly 86% of the total time.

3.4.2 | Temperature and state of charge

Temperature and SOC should be investigated to ensure that the pack is working within temperature limits and

without significant change and that the SOC is within recommended limits. Figure 11 shows temperature variation across the whole cycle.

The temperature range was between 16.5°C and 18°C. Figure 12 shows the SOC during the duty cycle.

3.5 | RE firming

3.5.1 | The reference signal tracking

Figure 13 shows the battery power response to the tracing power signal. The BP failed to complete the full

duty cycle due to reaching the SOC safety upper limit. Therefore, the battery was discharged out of the duty cycle with some rest time and then the duty cycle was completed.

The battery performed well, without any related issues when the SOC reached the maximum allowable limit. The reason for this is that the discharge energy was higher than the set point of the test. As mentioned earlier, the battery was tested without any modifications since the time it was retired from the car, and alterations, for example, such as

accessing the BMS and changing the maximum limits of the battery in terms of SOC and voltage could improve the battery's characteristics for use in grid applications.

The battery reached the maximum safety SOC set in the test parameters. The fail point is caused by the early full charge of the BP. However, if more battery cells/packs are added to the configuration, such problems can be avoided. This is a system sizing problem, and thus, for reuse of second-life batteries, in addition to the individual BPs, the management, size, connection structure, and charge balance

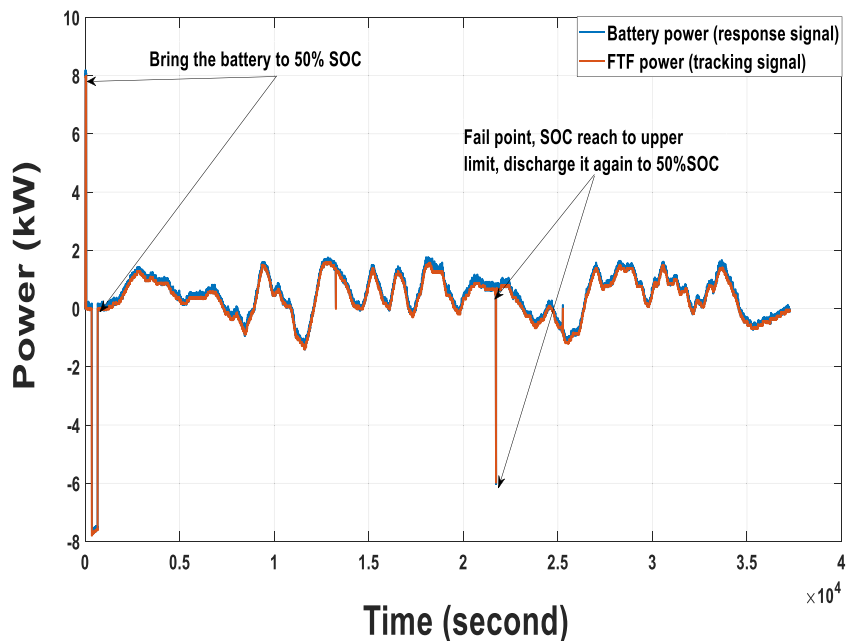


FIGURE 13 Battery power versus tracking the signal in renewable firming duty cycle

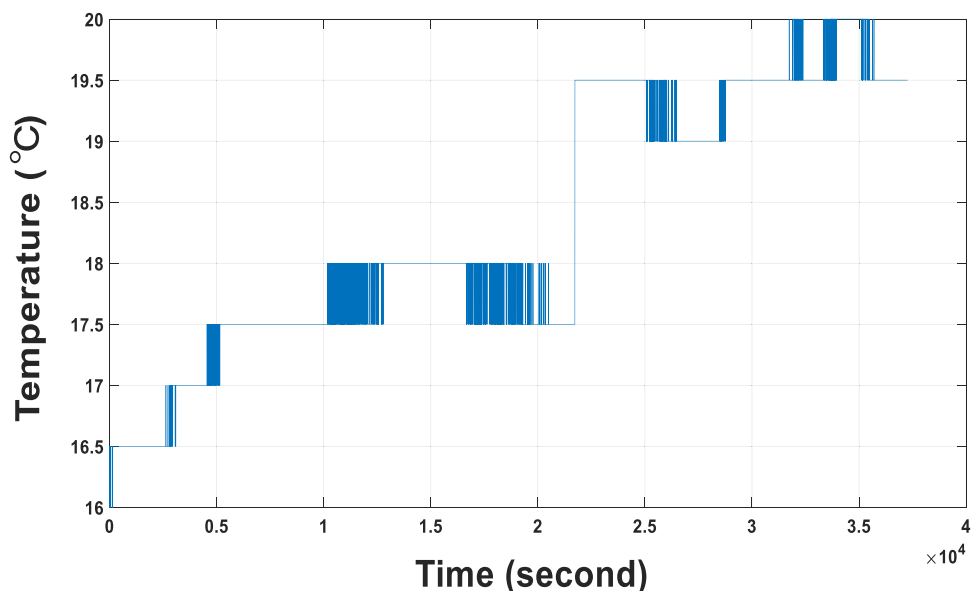


FIGURE 14 Temperature profile during the firming duty cycle

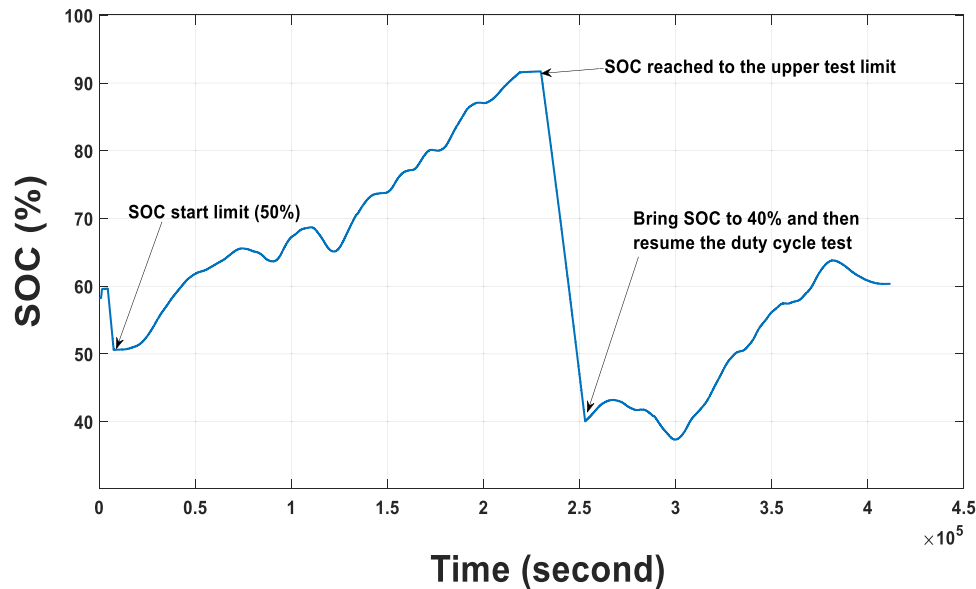


FIGURE 15 State of charge (%) profile during the firming duty cycle

of each BP are also important for system performance.^{21–23} In this study, increasing the number of cells in the battery was not possible. The percentage of nontracking time compared to the whole cycle was 11% (which was better than PV smoothing). However, this is still above the desired recommended limit of 2%. In terms of tracked time, the BP was tracked for nearly 8.9 h out of 10. In other words, there were nearly 1.1 h overall without tracking.

$$\% \text{ of time signal tracked} = (8.9 \div 10) \times 100 = 89\%.$$

The pack tracked the signal for nearly 89% of the total time.

3.5.2 | Temperature and state of charge

As in other duty cycles, the SOC and temperature needed to be investigated. Figure 14 shows the temperature profile during the firming duty cycle.

The temperature variation was between 16°C and 20°C. This is an acceptable range since the battery was run without temperature control or a proper cooling system. The SOC profile during PV firming is presented in Figure 15.

The battery failed to finish the whole duty cycle. After 6 h and 23 min, the battery reached the upper SOC and V_{\max} test limit, which was 340 V. This limit was set up to end individual stages of the test and run the next steps, without opening the safety contactors of the BMS. As a summary of this test, the battery shows similar characteristics to PV smoothing except for the SOC fail point and appears inadequate for this purpose.

4 | CONCLUSION

This study explores the potential to repurpose batteries first used for electric vehicles for applications in energy storage for power grids. The test started with the reference test to check the actual capacity of the pack. The reference test was performed under different C-rates 1 C, 0.5 C and C/5. The result showed that the BP was in a good condition, with no need to strip down the pack and conduct further tests at module or cell levels at this stage. It is important to consider the impact of temperatures on internal resistance, which is based on temperature and battery charge condition. Internal resistance is reduced as temperature rises, with variation also by charge state, in a possibly nonlinear relationship. When the current rate is high, while there is high overpotential, which could accordingly raise internal resistance, the high current also raises the temperature of cells, ultimately causing internal resistance to fall. Therefore, higher C leads to a lower average value for internal resistance for a cycle of charge/discharge. This explains the differences between the voltages and capacities during charge and discharge at the reference capacity test.

Then, four different grid applications were performed to determine the ability of the pack to fulfil the service. The results of these tests showed that the pack was showing the best performances during peak shaving applications, fully meeting the requirements of this service. The pack was also able to partly meet the requirements of FR. The untracking time for the whole signal was nearly 4% (slightly exceeding the condition of passing the tracking test, which is 2%). The SOC and temperature were within the permitted limits. The PV

firming and renewable energy smoothing services seem difficult to achieve with this pack. The untracking time for the whole signals was nearly 14% and 11% for PV smoothing and renewable energy (RE) firming, respectively (greatly exceeding the condition for passing the tracking test which is 2%). For the PV firming, the untracking time was quite high in contrast with the recommended level, although the SOC and temperature were within the permitted limits.

RE smoothing was the worst scenario. There was a fail point in the SOC limit since the battery was fully charged after 6 h and 23 min. However, the fail point appeared because the battery reached the maximum capacity, so adding more cells or increasing the battery size could overcome this issue. This is a system sizing problem, and thus for reuse of second-life batteries in addition to the individual BPs, BMS, pack size, connection and cabling structure, and the pack balancing during charge and discharge of each BP is also important for system performance.

These results suggest a number of directions for further research work, as well as supporting the development of second-life battery approaches to be commercially utilised. Going forward, tests should be based on a range of signals using recent sources that are in line with guidance for testing.

ACKNOWLEDGEMENTS

This study was funded by the European Regional Development Fund within the Smart Energy Storage Solutions Hub (SESS) scheme, led by the University of South Wales (USW). The responsibility for this publication rests with the authors.

CONFLICTS OF INTEREST

The authors declare no conflicts of interest.

DATA AVAILABILITY STATEMENT

The data used to support the findings of the study are included in the article. However, the corresponding author is happy to answer any enquires or questions regarding the article.

ORCID

Abdulla Rahil  <https://orcid.org/0000-0002-1848-159X>

Mian H. Nazir  <https://orcid.org/0000-0002-7623-0625>

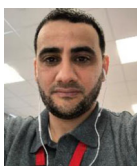
Muhammad M. Hussain  <https://orcid.org/0000-0002-6255-6966>

REFERENCES

- Zhu J, Mathews I, Ren D, et al. End-of-life or second-life options for retired electric vehicle batteries. *Cell Rep Phys Sci*. 2021;2:100537.
- Hoarau Q, Lorang E. An assessment of the European regulation on battery recycling for electric vehicles. *Energy Policy*. 2022;162:112770.
- Chen M, Ma X, Chen B, et al. Recycling end-of-life electric vehicle lithium-ion batteries. *Joule*. 2019;3:2622-2646.
- Mathews I, Xu B, He W, Barreto V, Buonassisi T, Peters IM. Technoeconomic model of second-life batteries for utility-scale solar considering calendar and cycle aging. *Appl Energy*. 2020;269:115127.
- Song Z, Feng S, Zhang L, Hu Z, Hu X, Yao R. Economy analysis of second-life battery in wind power systems considering battery degradation in dynamic processes: real case scenarios. *Appl Energy*. 2019;251:113411.
- Alhadri M, Zakri W, Farhad S. Second-life analysis of lithium-ion battery in a residential solar photovoltaic grid-tied system. Proceedings of the ASME 2021 IMECE; 2021; V08BT08A046.
- Deng X, Deng Z, Song Z, Lin X, Hu X. Economic control for a residential photovoltaic-battery system by combining stochastic model predictive control and improved correction strategy. *J Energy Resour Technol*. 2022;144(5):054501.
- Tong SJ, Same A, Kootstra MA, Park JW. Off-grid photovoltaic vehicle charge using second life lithium batteries: an experimental and numerical investigation. *Appl Energy*. 2013;104:740-750.
- Heymans C, Walker SB, Young SB, Fowler M. Economic analysis of second use electric vehicle batteries for residential energy storage and load-levelling. *Energy Policy*. 2014;71:22-30.
- Martinez-Laserna E, Gandiaga I, Sarasketa-Zabala E, et al. Battery second life: hype, hope or reality? A critical review of the state of the art. *Renew Sustain Energy Rev*. 2018;93:701-718.
- Madziga M, Rahil A, Mansoor R. Comparison between three off-grid hybrid systems (solar photovoltaic, diesel generator and battery storage system) for electrification for Gwakwani Village, South Africa. *Environments*. 2018;5:57.
- Barton JP, Gammon RJL, Rahil A. Characterisation of a nickel-iron battery, an integrated battery and electrolyser. *Front Energy Res*. 2020;8:1-15.
- Rahil A, Gammon R, Brown N. Techno-economic assessment of dispatchable hydrogen production by multiple electrolysers in Libya. *J Energy Storage*. 2018;16:46-60.
- Rahil A, Gammon R, Brown N. Dispatchable hydrogen production at the forecourt for electricity grid balancing. AIP Conference Proceedings, AIP Publishing; 2017:20011.
- Rahil A, Gammon R, Brown N, Udje J, Mazhar MU. Potential economic benefits of carbon dioxide (CO₂) reduction due to renewable energy and electrolytic hydrogen fuel deployment under current and long term forecasting of the Social Carbon Cost (SCC). *Energy Reports*. 2019;5:602-618.
- Delta Elektronika. 2019. Accessed May 15, 2018. <https://www.delta-elektronika.nl/en/products/bidirectional-dc-power-supplies-15kw-sm15k-series.html>
- Conover D, Ferreira SR, Crawford AJ, et al. Protocol for uniformly measuring and expressing the performance of energy storage systems. *Off Electr Deliv Energy Reliab*. 2016.
- Rosewater D, Ferreira S. Development of a frequency regulation duty-cycle for standardized energy storage performance testing. *J Energy Storage*. 2016;7:286-294.
- Thompson B. Repurposing electric vehicle batteries in a mixed array for grid storage. 2018. Accessed February 24, 2022. <https://dalspace.library.dal.ca/handle/10222/73868>

20. Ferreira SR, Rose DM, Schoenwald DA, et al. Protocol for uniformly measuring and expressing the performance of energy storage systems. *Off Electr Deliv Energy Reliab.* 2014;12:8-12.
21. Han W, Zou C, Zhou C, Zhang L. Estimation of cell SOC evolution and system performance in module-based battery charge equalization systems. *IEEE Trans Smart Grid.* 2018;10:4717-4728.
22. Rahimi-Eichi H, Ojha U, Baronti F, Chow MY. Battery management system: An overview of its application in the smart grid and electric vehicles. *IEEE Ind Electron Mag.* 2013;7:4-16.
23. Wik WHT, Kersten A, Dong G, Zou C. Next-generation battery management systems: dynamic reconfiguration. *IEEE Ind Electron Mag.* 2020;14:20-31.

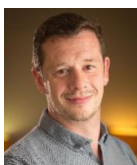
AUTHOR BIOGRAPHIES



Dr. Abdulla Rahil has a passion for renewable energy in the United Kingdom, delivered through electrical energy storage techniques. He has a strong background in energy storage and grid application. Abdulla is working as a battery test engineer in CAPSE at the University of South Wales. Abdulla completed his PhD in the School of Engineering and Sustainable Development at De Montfort University and his Masters at Tripoli University, Libya. He has also worked as a lecturer and research assistant in many projects at De Montfort University and the University of Leicester.



Mr. Eduard Partenie's passion for renewable energy technologies led him to study this subject at degree level, achieving a First Class Honours and a Certificate of Excellence Award. His research interests include the management systems of the battery packs for monitoring and equalising the state of charge of the cells. Eduard followed on to combine the theory with practical know-how and undertook an industrial placement as a Data Analyst for biomass plants and wind farms with ECO2. He also conducted energy assessments for community buildings in South Wales, worked with electricians at the University of South Wales and has mentored new students for over 4 years.



Mr. Mark Bowkett obtained his Master's degree in Electronic and communications at the University of Glamorgan now known as the University of South Wales. He went on to work for the university in the Centre of Electronic Product Engineering for 2 years designing and building products for small businesses. Leaving the academic

environment he went to work in industry for 3 years also in a product design role before returning to the University of South Wales. Currently, he works at the Centre of Automotive & Power Systems Engineering which has included a mix of roles including lecturing, research, student supervision, product design and testing of hybrid vehicle batteries systems.



Dr. Mian Hammad Nazir is currently working as a lecturer (assistant professor) at University of South Wales. Dr Nazir received BSc and MSc degrees in 2008 and 2011 from UET Taxila Pakistan and Jonkoping University Sweden respectively, and PhD degree in structural health monitoring from Bournemouth University in 2016. He worked as a senior research fellow in the University of South Wales from November 2018 till October 2021 with research focusing on batteries for future EVs. He worked as a post-doctoral research associate with the NanoCorr, Energy and Modelling Research Group, Bournemouth University, from January 2016 till November 2018. He has authored or co-authored over 50 publications and two patents in structural health monitoring and analysis with over 600 citations to date. Dr. Nazir has expertise in Lithium Cells/Modules/Batteries, Embedded Control Systems, Battery Management Systems (BMS) and Thermal Management Systems (TMS) for future EVs and Smart storage grid applications; Computational and numerical modelling; Thin films; Nanomaterials; Corrosion; Tribology; Smart Sensors; Research Excellence Framework (REF).



Dr. Muhammad Majid Hussain is a lecturer in the Electrical & Electronic Engineering Department at the University of South Wales, United Kingdom. He received the BSc degree from BZ University Multan, Pakistan in 2005 and MSc from UET, Lahore, Pakistan in 2009 and PhD degree from Glasgow Caledonian University, UK in 2018. His current research interests include High Voltage Technology, Smart Grid and Energy Management.

How to cite this article: Rahil A, Partenie E, Bowkett M, Nazir MH, Hussain MM. Investigating the possibility of using second-life batteries for grid applications. *Battery Energy.* 2022;20210001. doi:10.1002/bte2.20210001